University of Baghdad
College of Engineering
JE
JOURNAL OF ENGINEERING

Journal of Engineering

journal homepage: www.joe.uobaghdad.edu.iq

Volume 29 Number 5 May 2023

Experimental Evaluation of PV Panel Efficiency Using Evaporative Cooling Integrated with Water Spraying

Deyaa Mohammed Noori Mahmood *
Ph.D. student
Dept. of Mechanical Engr.
College of Engr.-Univ. of Baghdad
Baghdad, Iraq
E-mail: d.noori1003@coeng.uobaghdad.edu.iq

Issam M. Ali Aljubury
Assist. Prof., Ph.D
Dept. of Mechanical Engr.
College of Engr.-Univ. of Baghdad
Baghdad, Iraq
E-mail: drissam@uobaghdad.edu.iq

ABSTRACT

In this work, an inventive photovoltaic evaporative cooling (PV/EC) hybrid system was constructed and experimentally investigated. The PV/EC hybrid system has the prosperous advantage of producing electrical energy and cooling the PV panel besides providing cooled-humid air. Two cooling techniques were utilized: backside evaporative cooling (case #1) and combined backside evaporative cooling with a front-side water spray technique (case #2). The water spraying on the front side of the PV panel is intermittent to minimize water and power consumption depending on the PV panel temperature. In addition, two pad thicknesses of 5 cm and 10 cm were investigated at three different water flow rates of 1, 2, and 3 lpm. In Case #1, the evaporative cooling decreased the temperature of the PV panel by about 15 ℃ related to the uncooled PV panel for both pad thicknesses. While case #2 showed a more significant temperature drop for PV panel by about 27 ℃ and 29.7 ℃ for pad thicknesses of 5 cm and 10 cm, respectively. Compared to the uncooled PV panel, the cooled panel had a distinct enhancement in performance. The efficiency of the PV panel in case #1 was augmented by 5.7% with 50 mm pad thickness and 8.4% for 100 mm pad thickness. Case #2 revealed more improvement in the efficiency by 9% for 5 cm and up to 20% for 10 cm pad thickness. The PV panel electric power was augmented by 7.3% and 13.8% for 2 and 3 lpm water flow rates, respectively. Compared to the flow rate of 1 lpm. The open voltage circuit improved by 4.1% and 9.4% for cases #1 and #2, respectively. The higher air temperature drop was about 11.4 ℃ for case #2 at 10 cm pad thickness.

Keywords: PV panel, solar energy, evaporative cooling, spray cooling.

*Corresponding author
Peer review under the responsibility of University of Baghdad.
https://doi.org/10.31026/j.eng.2023.05.03

Article received: 31/10/2022
Article accepted: 02/04/2023
Article published: 01/05/2023

التقييم التجريبي لكفاءة الألواح الفوتوفولطائية باستخدام التبريد التبخيري المتكامل مع رش الماء

ضياء محمد نوري محمود*
طالب دكتوراه
جامعة بغداد– كلية الهندسة

عصام محمد علي الجبوري
استاذ مساعد, دكتوراه
جامعة بغداد–كلية الهندسة

الخلاصة

في هذه الدراسة، تم إنشاء نظام تبريد تبخيري فوتوفولطائي هجين مبتكر (PV / EC) ودراسته بشكل تجريبي. يتمتع نظام PV EC / الهجين بميزة مزدهرة في إنتاج الطاقة الكهربائية وتبريد اللوحة الكهروضوئية إلى جانب توفير هواء رطب مبرد. تم استخدام طريقتين للتبريد ؛ التبريد التبخيري الخلفي (الحالة رقم 1) ، والتبريد التبخيري الخلفي المشترك مع تقنية رش الماء الأمامي (الحالة رقم 2). يكون رش الماء على الجانب الأمامي من اللوحة الفوتوفولطائية بشكل متقطع لتقليل استهلاك المياه والطاقة اعتمادًا على درجة حرارة اللوحة الفوتوفولطائية. إضافة إلى ذلك ، تم اختبار سماكتين للحشوة السليلوزية 5 سم و 10 سم بثلاثة معدلات تدفق مختلفة للمياه 1 و 2 و 3 لتر في الدقيقة. في الحالة رقم 1 ، كان انخفاض درجة الحرارة حوالي 15 درجة مئوية للوحة الفوتوفولطائية المبردة مقارنة باللوحة غير المبردة لكلا سماكات الحشوة. بينما أظهرت الحالة رقم 2 أعلى انخفاض في درجة حرارة اللوحة الفوتوفولطائية بمتوسط قيم 27 درجة مئوية و 29.7 درجة مئوية لسماكات الحشوة 5 سم و 10 سم على التوالي. أظهرت النتائج تحسنًا في أداء اللوحة الفوتوفولطائية المبردة مقارنة باللوحة الفوتوفولطائية غير المبردة. حيث ازدادة كفاءة اللوحة الفوتوفولطائية في الحالة رقم 1 بنسبة 5.7٪ بسماكة 5 سم و 8.4٪ لسمك الحشوة 10 سم. اظهرت الحالة رقم 2 مزيد من التحسن في الكفاءة بنسبة 9٪ لـ 5 سم وما يصل إلى 20٪ لسمك الحشوة 10 سم. زادت قدرة اللوحة الفوتوفولطائية بنسبة 7.3٪ و 13.8٪ لمعدلات تدفق المياه 2 لتر في الدقيقة و 3 لتر في الدقيقة على التوالي مقارنة بمعدل التدفق البالغ 1 لتر في الدقيقة. كان التحسن في فولطية الدائرة المفتوحة بنسبة 4.1٪ و 9.4٪ للحالة رقم 1 والحالة رقم 2 على التوالي. كان اعلى انخفاض في درجة حرارة الهواء بحدود 11.4 درجة مئوية للحالة رقم 2 بسماكة 10 سم.

الكلمات الرئيسية: الألواح الفوتوفولطائية ، الطاقة الشمسية ، التبريد التبخيري ، التبريد بالرش.

1. INTRODUCTION

Photovoltaic PV systems are a technique used to convert sunlight into electric energy and harness the solar energy, the most significant forms of renewable energy. The system can be easily installed on residential buildings' rooftops and in large areas of power plants. Yet it still has a low conversion efficiency of less than 20% **(Qiu et al., 2022)**. A relatively small amount of solar irradiation that reaches the PV module is converted to electrical power. However, the overwhelming majority leads to heat up the panel, and this causes the efficiency to fall even further. PV panel efficiency experiences a reduction of roughly 0.3 to 0.5% for each increase of 1 °C in panel temperature **(Haidar et al., 2016)**. There are many

approaches for cooling PV modules, including active and passive methods. These include water-based, air-based, evaporation-based, and spray-based methods. Cooling with water is more efficient than air cooling because the water has higher thermal capacity **(Suresh and Shanmadhi, 2020)**. Among cooling techniques, evaporative cooling stands out as one of the most effective, particularly in arid areas, **(Haidar et al., 2018)**. It is widely used in domestic and industrial cooling applications but still receives limited attention in PV panel cooling and requires further study **(Haidar et al., 2021)**.

(Bahaidarah et al, 2013) carried out an experimental and theoretical assessment of a 230 W PV panel's performance, utilizing an active water-cooling method. A heat exchanger was installed on the PV module's backside. And passing cold water from an insulated tank through the heat exchanger using ½ hp water pump. The outcomes of the experiments exhibited an increase in the electrical efficiency of the PV unit by 9%. **(Nizetic et al., 2016)** sprayed water on the two faces of the PV module concurrently. The maximal enhancement (effective) in the power output and effectiveness was 7.7% and 5.9%, respectively. **(Schiro et al., 2017)** proposed adding a front-side water spray cooling arrangement onto conventional PV units (100 kW) to increase their output power without altering the existing panel structure. The electric power output was augmented by 5.5%. **(Ahmed and Danook, 2018)** used front-side water cooling with a flow rate ranging from 3 to 9 lpm, and the panel efficiency was augmented by 3.28% to 6.71%. **(Castanheira et al., 2018)** utilized a spray water cooling technique to cool a real PV power station (5 kW). The study showed that it could boost PV yearly output by 12%. **(Harahap et al., 2019)** installed a perforated tube on the upper edge of the photovoltaic panel's front side. The water was passed on the PV module's front side at a flow rate of 2.5 lpm. This resulted in drop in temperature by a mean value of 18.7°C and an increase in device efficiency by 8.6%. **(Bevilacqua et al., 2020)** investigated water spray and forced air ventilation in three cases. Water was sprayed on the rear side, same as in the first case, but now with an additional metal plate installed on the rear side of the PV unit, and forced air ventilation was by adding a perforated metal plate equipped with a fan on the PV module rear side. The maximum increment of power output was 6.1%. **(Suresh and Shanmadhi, 2020)** combined an evaporative cooling pad to a PV panel backside. A multi-point water inlet nozzle pipe was coupled to the PV module, and it was used to dampen the cooling pad. According to the study's findings, using the cellulose evaporative cooling pad improved power output by 6.8% on average.

(Risdiyanto et al., 2020) employed a water spray controller to regulate the PV module temperature at 30°C against the increasing temperatures above it. The PV module backside was moistened with water from 32 nozzles **(Almuwailhi and Zeitoun, 2021)** to investigate the forces and the free evaporative cooling (EC) of PV panels. The free cooling was accomplished by installing the panel on an insulated channel that contained a wetted fabric, and the air passed through the channel naturally. A small fan drove air through the channel during forced EC. Free and forced EC enhanced the panel's efficiency by 2.7% and 3.8%, respectively. **(Haidar et al., 2021)** conducted experimental investigation of the PV unit cooling using evaporative cooling. A PV module was set into a channel. Water flowed on a fabric placed on the bottom side of the duct. A fan was used to drive air within the duct. The PV panel temperatures fell by 10 ℃ while the power increased by 5%. A dual-surface cooling technique was employed by **(Agyekum et al., 2021)** to enhance the efficiency and the produced power of the PV unit. This included cooling the frontal face of the module with flowing water and the rear surface using a moist cotton wick mesh. As a

consequence, the temperature of the PV unit fell by 23.5 °C, while the electric efficiency was augmented by 11.9%. **(Kadhim and Aljubury, 2021)** proposed burying a water tank underground to keep the water cooled and then spraying that cold water to a cooling pad mounted on the PV panel's backside. Several cases were investigated, including; continuously and intermittently spraying water on the frontal side of the PV system. It employed four nozzles to spray water on the PV panel. The water flow rate was 3.5, 5, and 7 lpm. The temperature of the PV units fell with a round of 4 ℃ and 12.6 ^{0}C, while its efficiency increased by 1.74% to 16%. **(Mahdi and Aljubury, 2021)** cooled the PV panel by spraying underground water directly to the frontal side of the PV module. This led to a reduction in the temperature of the PV unit by 20 ℃. The electric power output of the PV module was augmented by 24%. **(Alktranee and Bencs, 2022)** investigated passive evaporating cooling by using cotton wicks that were immersed in the water and installed on the rear surface of the PV panel. The results exhibited a decrease in the PV panel's temperature by 22%, and this reduction led to an increase in the electric efficiency by 7.25%. **(Zhao et al., 2022)** investigated how spray cooling affects the PV panel at a high solar concentration ratio. According to their study, the PV panel system performance is strongly related to the water spray temperature. A temperature reduction of 10 ℃ in spray water could enhance the produced power by 7.3%, and the electric efficiency increased by 6.85%.

The present work has experimentally investigated the performance of an innovative photovoltaic merged with evaporative cooling (PV/EC) hybrid system. The new hybrid system provides a cool and humidified air source for domestic applications while simultaneously cooling the photovoltaic panels and producing electrical energy. Water flow rates of 1, 2, and 3 lpm were studied with two cellulose pad thicknesses of 50 mm and 100 mm. The hybrid system integrates PV panels and evaporative cooling used for summer cooling in arid and hot climates. In addition, the water spray cooling system was also integrated with PV/EC to cool the panel's front side with the backside evaporative cooling. The proposed spray cooling system runs intermittently when the panel temperature exceeds the specified operating value to Save water and reduce energy consumption.

2. EXPERIMENTAL SETUP

2.1 Description of the Experimental System

Fig. 1 displays the experimental test rig setup. It comprises two identical 150 W silicon monocrystalline photovoltaic (PV) panels. **Table 1**. provides additional technical information about the panels.

Figure 1. The apparatus used for conducting the experiments

To investigate the effect of temperature on PV panel efficiency under equivalent operating conditions, one PV panel was cooled, and the second panel was not cooled (reference panel).

Table 1. Characteristic of the PV panel.

Property	Value	Property	Value
Trade mark	SAKO	I_{sc} (A)	8.71
Power output (W)	150	V_{mp} (V)	18.5
Panel size (cm)	148.2×67×3.5	V_{oc} (V)	22.5
Number of cells	36	Weight of panel (kg)	11.7
I_{mp} (A)	8.11		

Five K-type thermocouples in each panel were utilized to measure the PV module temperature. They were mounted carefully on the PV panel's rear side at the positions demonstrated in **Fig. 2**.

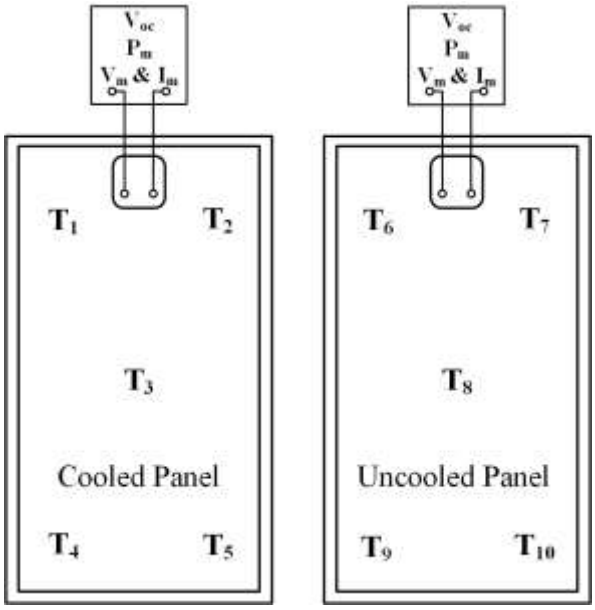

Figure 2. Locations of the thermocouples on the PV panels

The PV panel temperature used in comparisons is the middling value of the five measured temperatures. The thermocouples were insulated from the surrounding using a silicon strip and aluminum adhesive tape. The two PV panels were installed on the roof of a residential house in Baghdad city (33.3° N, 44.37° E) with an elevated of 3m with a 33.2° tilt angle toward the south. It considers Baghdad City's optimal annual tilt angle according to its latitudes **(Bailek et al., 2018)**. A cellulose paper pad was installed on the cooled PV module's backside, and then the assembled unit was put above an isolated metal channel. The specifications of the cellulose pads are given in **Table 2**.

The change in pressure across the cellulose pad was measured experimentally with a digital manometer, and it was about 20 Pa. The ambient hot air enters the evaporative cooling duct from the lower side, passes through the cooling pad, and exits the channel by

an axial, centrifugal fan model AKS-680-300 that is placed on the upper side of the evaporative cooling duct, as illustrated in **Fig. 3**. The fan has a maximum power consumption of 35 W, with an air flowrate of 225 m^3/hr, and a pressure drop of 63 Pa. A serpentine flexible perforation polyethylene tube is fixed on the pad to prevent bad water distribution, **Fig. 4**.

Table 2. Cellulose cooling pad characteristics.

Property	Value	Property	Value
Material	Cellulose	The angle of the corrugated sheet	45˚- 45°
Pad model	7090	The thickness of the sheet (mm)	0.2
The thickness of the pad (cm)	5, 10, 15	Height of corrugation (mm)	7
Height of the pad (cm)	148	The porosity of the pad	0.96
Width of the pad (cm)	67		

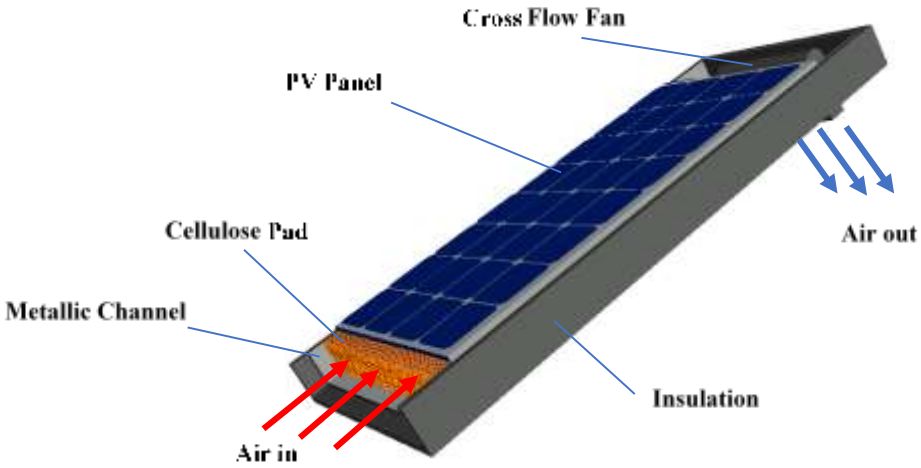

Figure 3. Schematic layout of PV/EC system.

The water dropped from the pad was collected in the basin placed under the cooling channel's entering. The basin is made of galvanized steel, well insulated, and has a capacity of 40 liters. A small 12-volt DC submersible water pump was placed into the basin to circulate the cold water between the basin and the evaporative cooling pad. The pump has a power of 19 W. The volume flow rate is 800 l/hr, and the pressure head of 5 m.

2.2 Spray Water System

The water spray system used in the present experimental work consists of the following parts; two nozzles, a booster water pump, and polyethylene tubes. The nozzles were fixed at the upper front side of the PV panel, as seen in **Fig. 5**.

The sprayed water was provided from the basin located under the PV panel, as the water pump took the water from the basin and pumped it to the nozzles to spray it on the PV module's front surface. The nozzle is shown in **Fig. 6**. It is a length of 27 mm and a width of 18 mm with a 6 mm tube diameter. The water pump is operated with 24-volt DC and a current not exceeding 1.2 A (28.8 W). This type of pump produced high pressure of 125 psi (861.8 kPa). The water flow rate of the pump is about 2 lpm, while the total measured

water flow rate of two nozzles was 0.2 lpm. The tubes used to connect the spray system equipment are made from PE material and have a diameter of ¼ and. This tube type is widely used in reverse osmosis RO systems and was chosen for its availability, ease of installation, handling, and cheapness. STC1000 controller with a temperature sensor was installed on the rear side of the PV panel. It was used to control the operation of the spray cooling system with on-off water, **Fig. 7**.

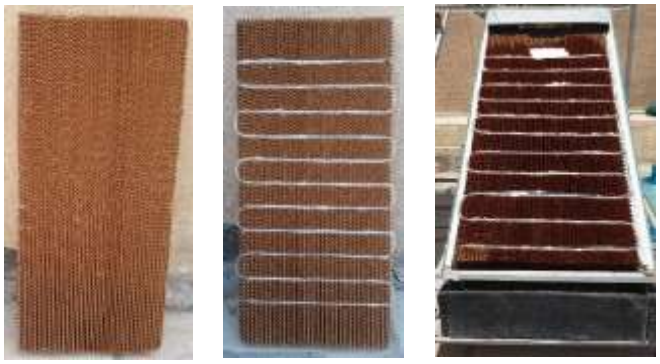

Figure 4. The arrangement of the water supply pipes and cellulose pad

Figure 5. Setups of water spray nozzles systems

Figure 6. Nozzle spraying water

Figure 7. Digital temperature controller

As the PV panel temperatures rise above the set value of 45 ℃, the pump will run, and when the temperature drops below 45 ℃, the pump will shut off. Different types of nozzles have been experimented with, and the one that was ultimately selected was based on the desired water droplet size. A smaller water droplet size would be unsuitable for this specific application because it would be dispersed by wind, resulting in reduced cooling efficiency and wastage of water. Conversely, a larger water droplet size would also decrease cooling efficiency and excessive water consumption.

3. TEST PROCEDURE

Fig. 8 depicts a schematic representation of the experimental test setup. Experiments were conducted in August from 9:00 to 15:00 on select sunny days. Before starting the test, the panels are cleaned of dust using an air blower. As an overview, the experimental test steps

are as follows. Initially, valve #1 has been opened to fill the water basin using municipal water. The water circulates through the EC system using primary water pump #1. As the water is pumping from the sink to the water distributed tube to damp the cooling pad. After that, the basin is filled with water that has fallen off the cooling pad. While the water consumption (evaporated) is compensated from a make-up water tank. Valve #2 and valve #3 were used to control the flowrate of water at 1, 2, and 3 lpm. A centrifugal cross-flow fan was utilized to drag the outside air in and pass it through the cooling pad. For case #2, when integrating the conventional PV/EC system with the water spray cooling, the spray system operates automatically based on the PV module surface's temperature. When the PV module temperature exceeds the designated operating temperature of 45℃, the water spray is turned on. The temperature controller (STC-1000) is set to stop the water spray when the panel's temperature drops by 0.5℃ below the operating temperature. The power, current, voltage, solar radiation, and relative humidity are measured each half hour, whereas the data logger recorded the temperatures each minute.

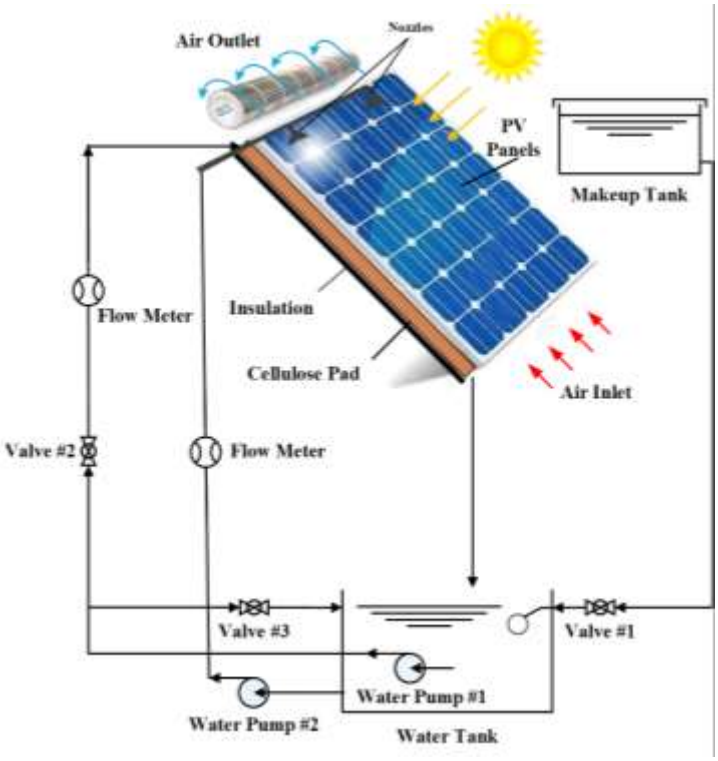

Figure 8. Schematic diagram of PV/EC with water spray system.

4. UNCERTAINTY ANALYSIS

Every experiment contains certain errors that need to be found. The uncertainty analysis aims to ensure that the earlier parts' outcomes are correct and unaffected by mistakes. Since the temperature reading is the most important variable in this investigation, the uncertainty was carried over. E_t represents the total error, and it is calculated as follows **(Thomas et al., 2011):**

$$E_t = \sqrt{E_p + E_B} \quad (1)$$

The bias error, E_B, is equal to 1 °C, as specified by the manufacturer. **Table 3** contains 8 temperature measurements from the same thermocouple, and Ep denotes the precision error determined from those measurements.

$$E_p = \frac{SD}{\sqrt{n}} t_{v,\frac{\varphi}{2}} \quad (2)$$

where *SD* refers to the standard deviation, *n* is the number of measurements, $t_{v,\varphi/2}$ is the t-distribution at the freedom degree *v=n-1*, with a 95% confidence level

Table 3. Measurements of Temperature for Precision Error (Ep) Calculation.

n	1	2	3	4	5	6	7	8
T (℃)	50.1	50.1	50.3	50.1	50.2	50.3	50.1	50.1

Then φ/2= 0.025, and from the table of the t-distributions, $t_{7,\,0.025}$=2.365, and the precision error E_p=0.0198 ℃, then the total error E_t=1.00039 ℃. The temperature difference observed during the experiments is more precise than the overall error. Therefore, the experimental results can be regarded as reliable and accurate.

5. POWER OUTPUT AND EFFICIENCY OF PV PANEL

To evaluate the impact of the two cooling cases on PV panel performance, three key parameters have been identified (power output, PV panel efficiency, and open circuit voltage). Experimental test conditions included the same air and water flow rate and pad thickness of 50 mm. The experiments were conducted on close days so that ambient temperature and solar radiation were as similar as possible when comparing cooling cases. Two panels were tested simultaneously for each case; one cooled and the other uncooled (reference panel). The efficiency represents the ratio of electric power produced by the PV panel to the incident solar radiation to the panel and can be calculated using Eq. (3) **(Sainthiya et al., 2018)**:

$$\eta = \frac{P}{G \times A} \quad (3)$$

Where η represents the efficiency of the PV panel that was measured experimentally, P is the electric power output (W), G is the incident solar radiation (W/m^2), and A the front surface area of the PV panel (m^2).

Eq. (4) is used to calculate the percentage improvement in PV panel efficiency **(Haidar et al., 2018)**:

$$\Delta\eta = \frac{\eta_c - \eta_{ref}}{\eta_{ref}} \times 100\% \quad (4)$$

where: $\Delta\eta$ is the enhancement efficiency ratio, η_c represents the efficiency of the cooled PV panel, and η_{ref} is the efficiency of the uncooled reference PV panel.
The temperature difference of the PV panel (ΔT_{panel}) is determined by Eq. (5)

$$\Delta T_{panel} = T_{ref} - T_c \quad (5)$$

Tc represents the cooled PV module temperature and Tref refers to the uncooled PV module temperature. The air temperature drop (ΔT_{air}) is computed as

$$\Delta T_{air} = T_{in,db} - T_{out,db} \quad (6)$$

where $T_{in,db}$ represents the dry bulb temperature of the air inlet, while $T_{out,db}$ is the dry bulb temperature of the air outlet.
The difference in the electric power (ΔP) is determined by Eq. (7) **(Almuwailhi and Zeitoun, 2021).**

$$\Delta P = P_c - P_{ref} \quad (7)$$

Pc refers to the electric power produced by the PV panel when it is cooled, while Pref refers to the output power of the PV panel when it is not cooled.

6. RESULTS AND DISCUSSION

6.1 Temperatures Changes

The temperature variation over the daytime for uncooled and cooled PV panels is shown in **Figs. 9** to **11** for two cooling test cases with two pad thicknesses for each case. The red curve reveals a gradual increase until reaching peak value at noontime, then decreasing. The blue line exhibit similar behavior to the red curve but in less extent for backside evaporative cooling (case #1). It showed different behavior when integrating with water spray cooling (case #2). The red and blue dashed lines represent the uncooled and cooled PV panels' average temperature. The ambient air temperature, represented by the black line, gradually increased from 9 AM to 3 PM during the test period. The exit air temperature (or supply air), shown by the green curve, remained relatively stable throughout the daytime, with only slight fluctuations. The air temperature difference represents the contrast between the inlet air temperature (ambient temperature) and the outlet air temperature (supply air).

6.1.1 Impact of Backside Evaporative Cooling

Fig. 9 illustrates the temperature variation over a day for backside evaporative cooling using a 50 mm-thick pad (case #1). During the testing day, the non-cooled PV unit temperature rises gradually, reaching a peak of 77℃, before declining to 64℃ at 3:00 PM. The cooled PV module followed a similar pattern, with the temperature increasing to a maximum of 59 ℃ at noon before decreasing to 52 ℃. This behavior can be attributed to several factors, with solar radiation being the primary factor. The radiation gradually increased until it peaked at noon and then declined. Also noticed is that the uncooled PV panel's temperature fluctuated due to the surrounding effects, in contrast to the cooled panel, whose temperature was more stable because of the evaporative cooling. The average uncooled and cooled panel temperature values were 69.8 and 54.7 ℃, respectively. The ambient air temperature increased gradually with test time and ranged between 40 to 48℃.

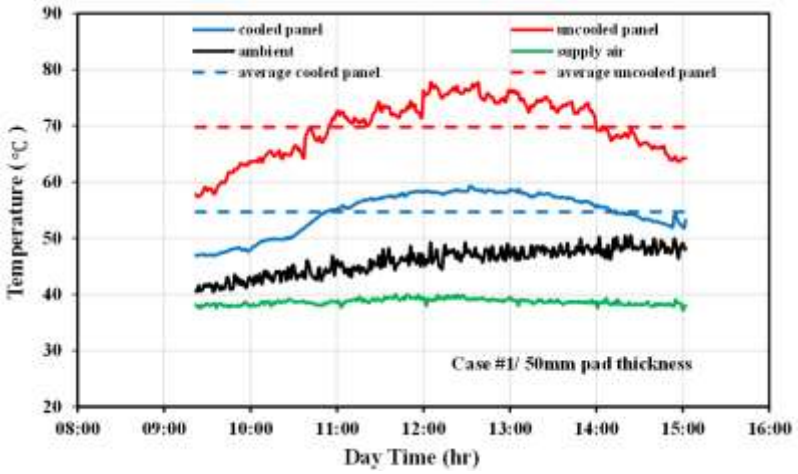

Figure 9. Temperature variation with time for case #1 with 50 mm pad thickness and 3 lpm water flowrate

Fig. 10 shows the temperature variation with time for case #1 with 100 mm pad thickness and 3 lpm water flow rate. The temperature curves exhibited similar behavior to that when using 50 mm pad thickness. The highest and average temperatures of the uncooled PV module were 70.4 and 64.2 °C, respectively. The surface temperature of the cooled PV module did not surpass 52 °C. The average temperature for the cooled PV panel was 49.2 °C. This indicates a gap of 15 °C in the temperature of the cooled and uncooled panels. The temperature of the surrounding air varied between 37°C and 46°C. While the supplied air temperature was almost constant within 34 °C.

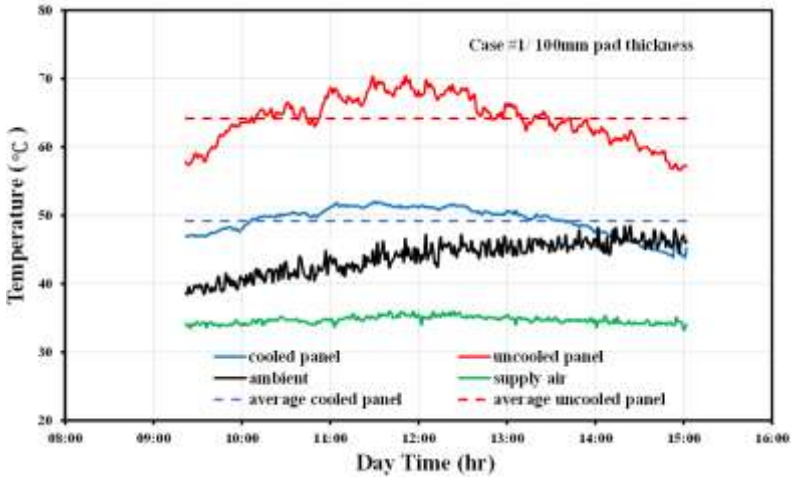

Figure 10. Temperature variation with time for case #1 with 100 mm pad thickness and 3 lpm water flowrate

6.1.2 Water Spray Cooling for PV Panel

Fig. 11 shows the temperature variation over time when employing water spray cooling on the front side of the PV panel and backside evaporative cooling using a 50 mm pad. The

temperature for the PV module that wasn't cooled was elevating and peaked at noon before decreasing. This behavior can be attributed to the impact of incident solar radiation, as previously mentioned. Also, the cooled PV panel temperature changes periodically because of the water spray cooling. When the temperature of the cooled PV module is elevated above a set value of 45 ℃. The water is sprayed on the PV panel's front side to decrease its temperature below 45℃. The temperature continues decreasing even after stopped the spray of water. Because the water remaining on the PV panel's front surface will be evaporated and absorb the heat from it. Also, in **Fig. 11,** the highest temperature of the uncooled PV panel was 76.4 ℃, the average value being 70 ℃. In this case, the cooled PV module recorded more temperature drop because of the added spray water cooling, as the panel temperature ranged between 36.7 ℃ to 48.2 ℃, and the average value was 43 ℃. It can also be noticed that the temperature of the cooled PV module is lower than the ambient air temperature. When using a pad thickness of 100 mm, the peak temperature of the uncooled PV module was 77.5 ℃ the average value being 70.2 ℃ as shown in **Fig. 12**. While the cooled

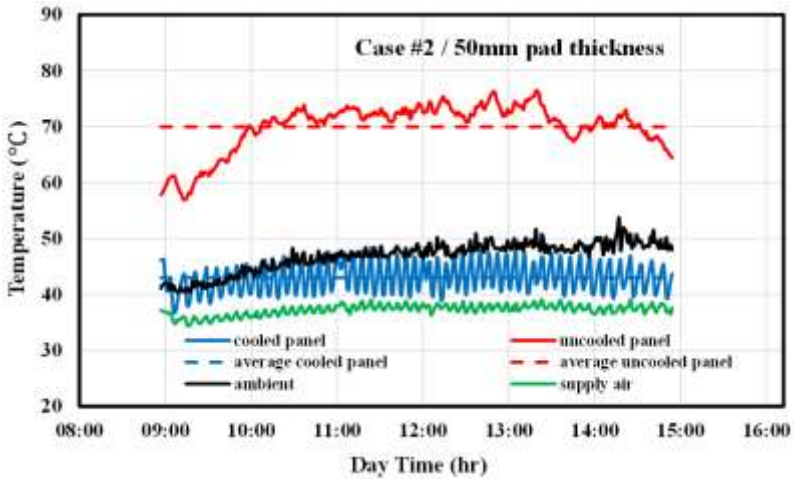

Figure 11. Temperature variation with time for case #2 with 50 mm pad thickness

panel temperature ranged between 33.3 ℃ to 45.6 ℃ and the middling value was 40.5 ℃. The cooled PV panel temperature using 100 mm pad thickness is lower than 50 mm pad thickness. The supplied air temperature was within 34 ℃ for 50 mm pad thickness and 30 ℃ for 100 mm pad thickness due to the rising pad thickness.

6.2 Comparison of Panel Temperature Drop for Two Cooling Cases

Fig. 13 presents the average and maximums temperature drop between the cooled and uncool the PV panel ed PV panels ($T_{uncooled\ PV} - T_{cooled\ PV}$) for case #1 and case #2. In case #1, the temperature dropped by 15.1 ℃ as the average value for the temperatures of the daytime hours. While in Case #2, the temperature decreased by 27 ℃, as the evaporative cooling was assisted by spray water. The maximum temperature dropped over the daytime was 18.6 ℃ and 28.2 ℃ for case #1 and case #2, respectively. The reduction in the temperature of the cooling PV panel for case #2 is more significant than case #1, whether for the maximum or average value. This is due to the assisted cooling by spraying water on the front side of the PV module in addition to the rear evaporative cooling.

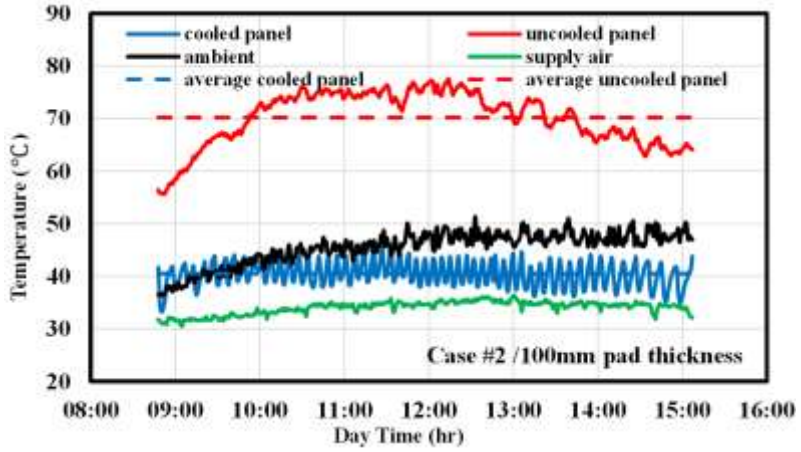

Figure 12. Temperature variation with time for case #2 with 100 mm pad thickness

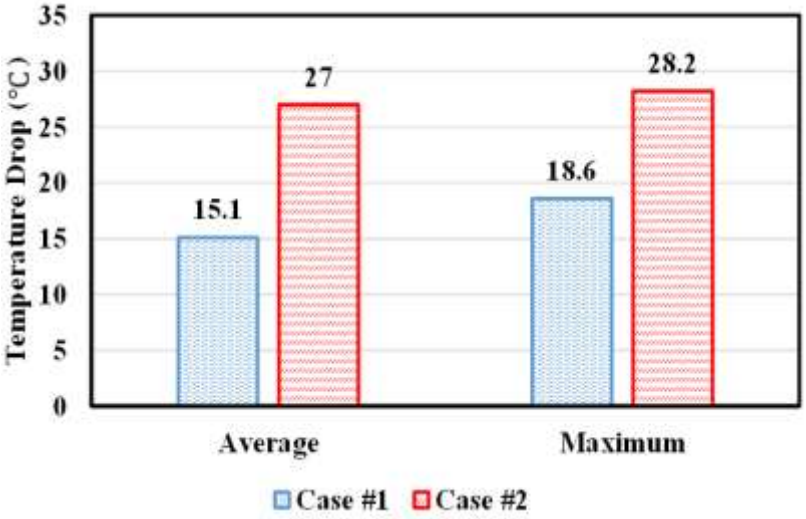

Figure 13. Temperature comparison of two cooling cases #1 and #2

Figs. 14 to **17** show the variation of the electric power output and the efficiency of the PV module, in addition to the solar radiation with time. It can be noticed that both the solar radiation and power output curves exhibit a comparable pattern, gradually rising and peaking at noon before declining. This indicates the strong effect of solar irradiation on power output. While the PV panel efficiency exhibited the opposite behavior, the efficiency decreased slightly, reaching the minimum value at noon and increasing. The explanation for this behavior is that the efficiency is directly proportional to power output and inversely to solar radiation. Since solar radiation changes intensely during the daytime, on the contrary, the output power changes less. Also, the panel temperature was at its peak value at noon time which led to a decrease in the efficiency of the PV panel

Fig. 14 shows the variation of the power output for the cooled and uncooled PV panel with time; for case #1, the power produced by the cooled panel increased gradually until reaching the peak value of 96 W. The average output power value of cooled and uncooled PV panels was 85.6 W and 81.2 W, respectively, at average solar radiation of 1019 W/m^2. Fig. 14 plotted the cooled and uncooled PV panels' efficiencies against time. The efficiency for the cooled panel was 8.3%, while the uncooled panel had an efficiency of 7.7%. Both

curves showed a slight decrease in efficiency at noon before increasing again. On average, the cooled panel showed a 5.7% improvement in efficiency compared to the uncooled PV module.

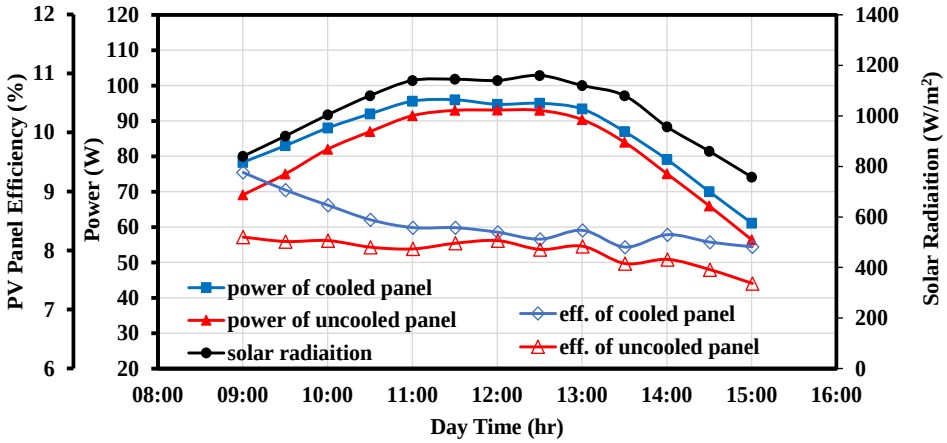

Figure 14. Variation of power output, efficiency, and solar radiation with time for case #1 with 50 mm pad thickness

In **Fig. 15**, the power output, PV panel efficiency, and solar radiation were plotted against time for case #1 with 100 mm pad thickness. The cooled panel had a maximum power output of 106 W at noon, with an average of 95.6 W. An increase of 8.4% in the produced power of the cooled panel was observed, as compared to the uncooled module, with a maximum power difference of 10 W between them.

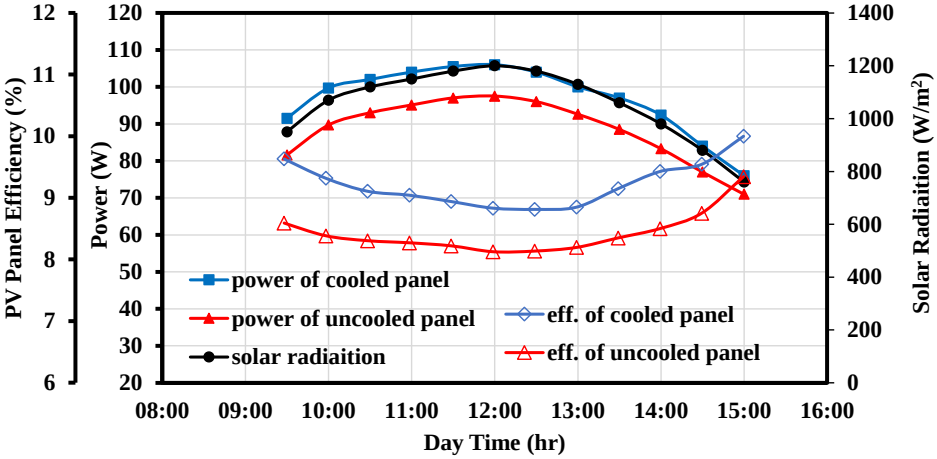

Figure 15. Variation of power output, efficiency, and solar radiation with time for case #1 with 100 mm pad thickness

In **Fig. 16**, the electric output power, PV module efficiency, and solar radiation were plotted against time for case #2 for a 50 mm thick pad. The cooled panel's power output reached a maximum of 98.2 W at noon and then decreased, while the maximum power change between the cooled and uncooled PV modules was 10.2 W. The cooled panel exhibited an efficiency of 9% greater than the uncooled panel. In **Fig. 17**, for case #2 with 100 mm pad thickness, the cooled panel achieved a maximum power output of 109 W at noon, with a

power difference of 22.1 W observed between the cooled and uncooled modules. On average, the cooled PV panel demonstrated a 20% improvement in efficiency when compared with the uncooled panel.

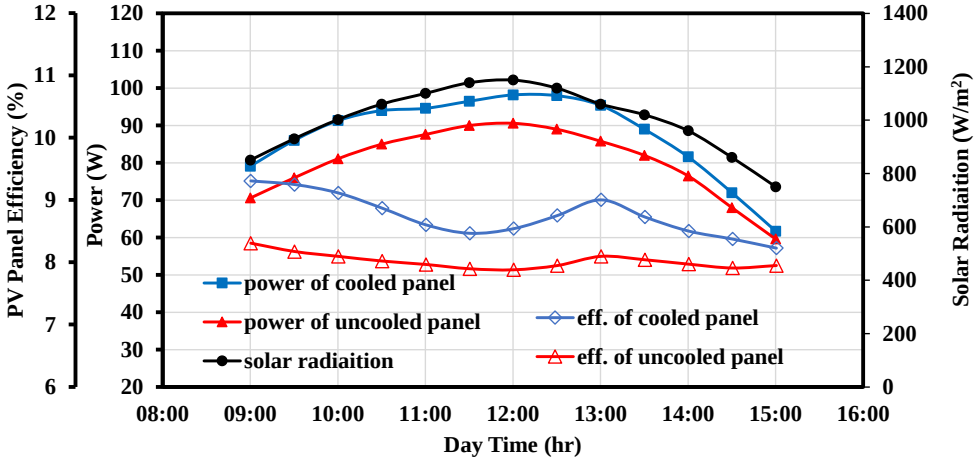

Figure 16. Variation of power output efficiency and solar radiation with time for case #2 with 50 mm pad thickness

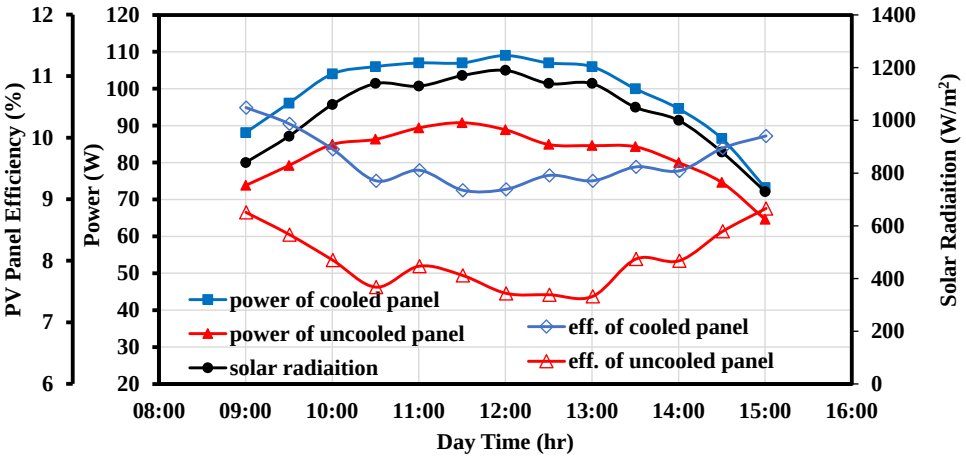

Figure 17. Variation of power output, efficiency, and solar radiation with time for case #2 with 100 mm pad thickness

6.3 PV Panel Open Circuit Voltage

The open circuit voltage (V_{OC}) is an important parameter to assign the performance of the PV unit and it is greatly affected by temperature, when the temperature of the PV panel rises the voltage drops. **Fig. 18** presents the variation of V_{OC} with daytime for cooled and non-cooled PV modules for both cases modules and two pad thicknesses (50 and 100 mm). In all cases, the V_{OC} of the cooled PV module is higher than that of the uncooled PV module. The V_{OC} of case #1 is lower than that of case #2, and the V_{OC} using 100 mm pad thickness is higher than that of 50 mm pad thickness. The average values of the V_{OC} for cooled PV panels are 20.3 V, 20.6 V, 20.8 V, and 21.2 V for case #1 with 50 mm, case #1 with 100 mm, case #2 with 50 mm, and case #2 with 100 mm pad thickness respectively. Case #2 with 100

pad thickness shows greater enhancement with an average value of 10.9%, while case #1 with 50 mm pad thickness has lower improvement with an average value of 4%.

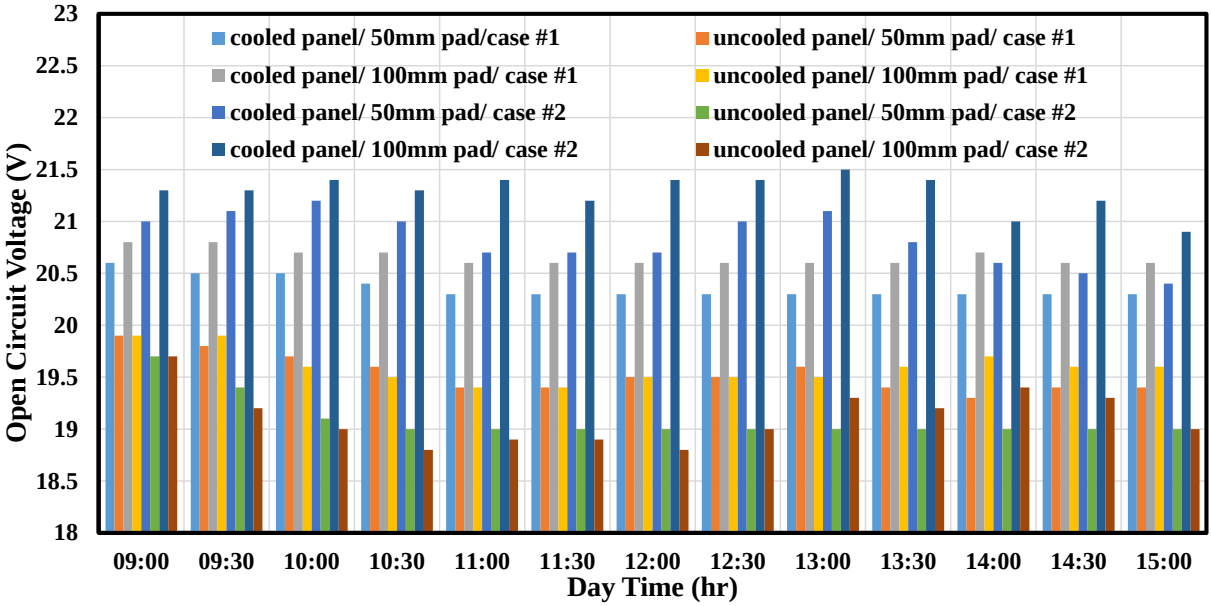

Figure 18. Variation of open circuit voltage of PV panel with time

6.4 Effect of Water Flowrate

The study examined the impact of water flow rate on the electric output power of PV modules, and this effect is demonstrated in **Figs. 19** and **20** for pad thicknesses of 50 mm and 100 mm, respectively. The researchers discovered that a rise in water flow rate increased power output. For the 50 mm pad thickness, **Fig. 19** demonstrates a progressive rise in electric power output as the water flow rate rose. The output power increased by an average of 7.3% and 13.8% for flowrates of 2 lpm and 3 lpm, respectively, compared to a flow rate of 1 lpm that produced 75.2 W output. Furthermore, all figures demonstrate a consistent increase in power output throughout the day, with a peak at midday and a decline due to the impact of decreasing solar radiation.

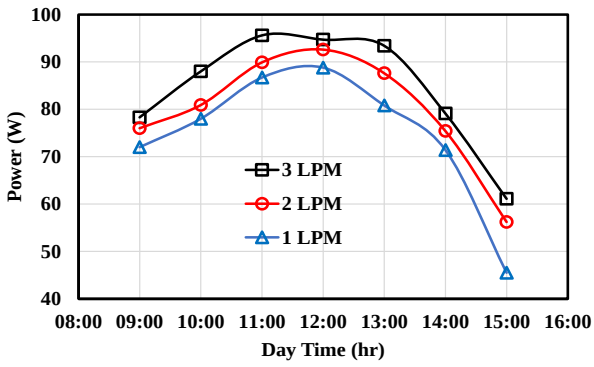

Figure 19. Influence of water flow rate on on the produced power of PV module using using 50 mm thick pad

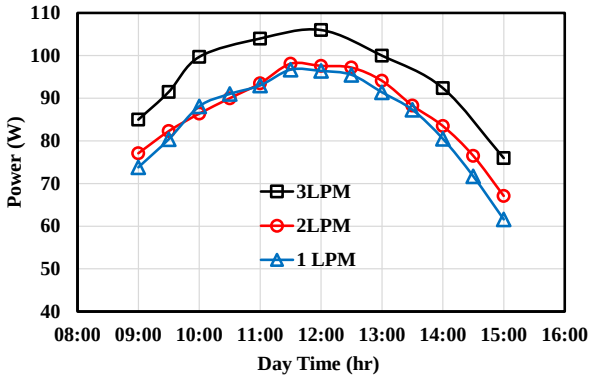

Figure 20. Influence of water flowrate the produced power of PV module 100 mm thick pad

These results suggest that a higher water flow rate can significantly augment the output power of the PV modules, particularly for thicker pads.

6.5 Comparison with the Previous Studies

Compared with previous studies on a cooling technique based on water and evaporative cooling, such as active, spray, and evaporative cooling. The parameters used for comparison are the temperature reduction of the PV module and the electric efficiency of the PV module. The comparison of PV panel temperature and the efficiency of the PV module is presented in **Table 4**. Case #2 (backside evaporative cooling with front-side water spray) with 50 mm and 100 mm thick pads were selected for comparison. The temperature reduction for the PV module in the present work is higher than in the previous studies. The efficiency of the PV unit for a 50 mm thick pad is similar to that obtained in the previous studies. While the efficiency of the PV unit for a 100 mm thick pad is higher than that of the previous studies. In addition, the current hybrid system is superior to previous systems by producing cold and humid air, cooling the PV panel, and generating electricity.

Table 4. Comparison with the previous studies

References	Cooling Technique	Temperature Reduction	Efficiency
(Risdiyanto et al. 2020)	Spray water cooling	21.85 ℃	9.03%
(Almuwailhi and Zeitoun, 2021)	Forced evaporative cooling	12.5 ℃	3.8%
(Bahaidarah et al., 2013)	Active water cooling	20 ℃	9%
Present study	Evaporative (50 mm pad thickness) and spray water cooling	27 ℃	9%
	Evaporative (100 mm pad thickness) and spray water cooling	29.8 ℃	20%

6. CONCLUSION

Two cooling techniques were tested for cooling the PV panel. Evaporative cooling (EC) was used in case #1, while water spray techniques were combined with evaporative cooling in case #2. The EC was accomplished by installing a cellulose pad on the PV panel's backside. The study tested two pad thicknesses, 50 mm, and 100 mm, with varying water flow rates of 1, 2, and 3 lpm. For case #2, the water spray cooling runs intermittently when the temperature of the PV panel exceeds the specified operating temperature (45 ℃), to reduce the water consumed. In case #1, only the back side of the PV module was cooled, whereas in case #2, Cooling was implemented on the PV panel's frontal and dorsal sides. The main results can be summarized in the following points:

- The average PV panel temperature decreased by 15.1 ℃ and 27 ℃ for cases #1 and #2, respectively, at a 50 mm thick pad.

- The electric efficiency of the PV unit was improved by 5.7% and 8.4% for pad thicknesses of 50 and 100 mm, respectively, with the implementation of backside evaporative cooling.
- By implementing a spray water cooling system (case #2), the efficiency of the PV unit was improved by 9% and 20% for pad thicknesses of 50 mm and 100 mm, respectively, in the hybrid PV/EC system.
- Increasing the pad thickness improves the PV module's EC and enhances the PV panel's power output and electric efficiency.
- Increasing the water flow rate from 1 lpm to 2 and 3 lpm improves the output power of the PV panel by 7.3% and 13.8%, respectively.
- The open voltage circuit V_{OC} was improved by 4.1% and 9.4% for case #1 and case #2, respectively.
- The reduction in air temperature was 7.2 ℃ and 9.2 ℃ for case #1 with pad thickness of 50 and 100 mm, respectively, and for case #2 with pad thickness of 50 and 100 mm, the temperature reduction was 9.6 ℃ and 11.4 ℃ respectively.

NOMENCLATURE

A = area, m^2
E_B = bias error
E_p = precision error
E_t = total error
G = solar irradiation, W/m^2
I_{mp} = current at maximum power, A
I_{sc} = current of the short circuit, A
P = electric power, W
P_m = maximum power point, W
PV = photovoltaic
PV/EC = photovoltaic evaporative cooling
SD = standard deviation
T = temperature, ℃
$T_{in,db}$ = dry bulb temperature of the inlet air, ℃
$T_{out,db}$ = dry bulb temperature of the outlet air, ℃
V_{mp} = voltage on the maximum power, V
V_{OC} = voltage of the open circuit, V
Δη = percentage enhancement efficiency, %
ΔT_{panel} = temperature drop of PV panel, ℃
ΔT_{airl} = temperature drop of the air, ℃
ΔP = electric power difference, W
η = PV panel efficiency, %

Subscripts

c= cooled
Ref= reference (uncooled)

REFERENCES

Agyekum, E. B., Kumar, S. P., Alwan, N. T., Velkin, V. I., and Shcheklein, S. E., 2021. Effect of dual surface cooling of solar photovoltaic panel on the efficiency of the module: experimental investigation. *Heliyon*, 7(9), p. 07920. doi:10.1016/j.heliyon.2021.e07920

Ahmed, A. M. and Danook, S. H., 2018. Efficiency improvement for solar cells panels by cooling. *2nd International Conference for Engineering, Technology and Sciences of Al-Kitab, ICETS 2018*. IEEE, (May), pp. 39–42. doi:10.1109/ICETS.2018.8724625

Alktranee, M. and Bencs, P., 2022. Effect of Evaporative Cooling on Photovoltaic Module Performance. *Process Integration and Optimization for Sustainability*, 6, pp. 921-930. doi.org/10.1007/s41660-022-00268-w

Almuwailhi, A. and Zeitoun, O., 2021. Investigating the cooling of solar photovoltaic modules under the conditions of Riyadh. *Journal of King Saud University - Engineering Sciences*, 35(2), pp. 123-136. doi:10.1016/j.jksues.2021.03.007

Bailek, N., Bouchouicha, K., Aoun, N., EL-Shimy, M., Jamil, B., and Mostafaeipour, A., 2018. Optimized fixed tilt for incident solar energy maximization on flat surfaces located in the Algerian Big South. *Sustainable Energy Technologies and Assessments*, 28, pp. 96–102. doi:10.1016/j.seta.2018.06.002

Bevilacqua, P., Bruno, R. and Arcuri, N., 2020. Comparing the performances of different cooling strategies to increase photovoltaic electric performance in different meteorological conditions. *Energy*, 195, p. 116950. doi:10.1016/j.energy.2020.116950

Bahaidarah, H., Subhan, A., Gandhidasan, P., and Rehman, S., 2013. Performance evaluation of a PV (photovoltaic) module by back surface water cooling for hot climatic conditions. *Energy*, 59, pp. 445-453. doi:10.1016/j.energy.2013.07.050

Castanheira, A. F. A., Fernandes, J. F. P. and Branco, P. J. C., 2018. Demonstration project of a cooling system for existing PV power plants in Portugal. *Applied Energy*, 211, pp. 1297–1307. doi:10.1016/j.apenergy.2017.11.086

Elghamry, R. and Hassan, H., 2020. Impact a combination of geothermal and solar energy systems on building ventilation, heating and output power: Experimental study. *Renewable Energy*, 152, pp. 1403–1413. doi:10.1016/j.renene.2020.01.107

Fernandes, F. T., Farret, F. A., Longo, A., Nardin, C. R., and Trapp, J. G., 2014. PV efficiency improvement by underground heat exchanging and heat storage. in *3rd Renewable Power Generation Conference (RPG 2014)*, pp. 1–6.

Haidar, Z. A., Orfi, J., Oztop, H. F., and Kaneesamkandi, Z., 2016. Cooling of solar PV panels using evaporative cooling. *Journal of Thermal Engineering*, 2(5), pp. 928–933. doi:10.18186/jte.72554

Haidar, Z. A., Orfi, J. and Kaneesamkandi, Z., 2018. Experimental investigation of evaporative cooling for enhancing photovoltaic panels efficiency. *Results in Physics*. , 11, pp. 690–697. doi:10.1016/j.rinp.2018.10.016

Haidar, Z. A., Orfi, J. and Kaneesamkandi, Z., 2021. Photovoltaic panels temperature regulation using evaporative cooling principle: Detailed theoretical and real operating conditions experimental approaches. *Energies*, 14(1), 145. doi:10.3390/en14010145

Harahap, H. A., Dewi, T. and Rusdianasari, 2019. Automatic Cooling System for Efficiency and Output Enhancement of a PV System Application in Palembang, Indonesia. *Journal of Physics: Conference Series*, 1167(1), 012027. doi:10.1088/1742-6596/1167/1/012027

Bahaidarah, H. M., Rehman, S., Gandhidasan, P., and Tanweer, B., 2013. Experimental evaluation of the performance of a photovoltaic panel with water cooling. *2013 IEEE 39th Photovoltaic Specialists Conference (PVSC)*, pp. 2987-2991, IEEE. doi:10.1109/PVSC.2013.6745090

Kadhim, A. M., and Aljubury, I. M. A., 2021. Experimental performance of cooling photovoltaic panels using geothermal energy in an arid climate. *Heat Transfer*, 50(3), pp. 2725–2742. doi.org/10.1002/htj.22002

Mahdi, A. H. and Aljubury, I. M., 2021. Experimental investigation of two-stage evaporative cooler powered by photovoltaic panels using underground water. *Journal of Build. Engineering*, 44, p. 102679. doi:10.1016/j.jobe.2021.102679

Nizetic, S., Coko, D., Yadav, A., and Grubisic-Cabo, F., 2016. Water spray cooling technique applied on a photovoltaic panel: The performance response. *Energy Conversion and Management*, 108, pp. 287–296. doi: 10.1016/j.enconman.2015.10.079.

Qiu, T., Wang, L., Lu, Y., Zhang, M., Qin, W., Wang, S., and Wang, L., 2022. Potential assessment of photovoltaic power generation in China. *Renewable and Sustainable Energy Reviews*, 154, 111900. doi:10.1016/j.rser.2021.111900

Risdiyanto, A., Kristi, A. A., Susanto, B., Rachman, N. A., Junaedi, A., and Mukti, E. W., 2020. Implementation of Photovoltaic Water Spray Cooling System and Its Feasibility Analysis. *Proceedings - 2020 International Conference on Sustainable Energy Engineering and Application: Sustainable Energy and Transportation: Towards All-Renewable Future, ICSEEA 2020*, pp. 88–93. doi:10.1109/ICSEEA50711.2020.9306133

Sainthiya, H., Beniwal, N. S. and Garg, N., 2018. Efficiency improvement of a photovoltaic module using front surface cooling method in summer and winter conditions. *Journal of Solar Energy Engineering, Transactions of the ASME*, 140(6), pp. 1–7. doi:10.1115/1.4040238

Schiro, F., Benato, A., Stoppato, A., and Destro, N., 2017. Improving photovoltaics efficiency by water cooling: Modelling and experimental approach. *Energy*, 137, pp. 798–810. doi:10.1016/j.energy.2017.04.164

Suresh, M. and Shanmadhi, R., 2020. Studies on the performance of 150W solar photovoltaic module with evaporative cooling. *IOP Conference Series: Materials Science and* Engineering, 912, (4), 042016. doi:10.1088/1757-899X/912/4/042016

Beckwith, T.G., Marangoni, R.D., and Lienhard, J.H., 2011. *Mechanical measurements*, Pearson Learning Solutions, 6th ed.

Zanlorenzi, G., Szejka, A. L. and Canciglieri, O., 2018. Hybrid photovoltaic module for efficiency improvement through an automatic water cooling system: A prototype case study. *Journal of Cleaner Production*, 196, pp. 535–546. doi:10.1016/j.jclepro.2018.06.065

Zhao, Y., Gong, S., Zhang, C., Ge, M., and Xie, L., 2022. Performance analysis of a solar photovoltaic power generation system with spray cooling. *Case Studies in Thermal Engineering*, 29, p. 101723. doi:10.1016/j.csite.2021.101723